Statics of Magnetic Bead Chain in Magnetic Field

Nobuyuki Nakayama, Hiroyuki Kawamoto✦ and Makoto Yamaguchi

Department of Mechanical Engineering, Waseda University, Shinjuku, Tokyo, Japan

Experimental, numerical, and theoretical investigations have been carried out on statics of a magnetic bead chain in the magnetic field. Chains formed on a solenoid coil were observed and chain lengths and slant angles were measured by a digital microscope. It was deduced that (1) the chain length depends on both the surface loading of magnetic particles and the magnetic flux density, and is almost independent of the particle diameter if the sufficient amount of particles are provided; (2) chains incline in the inclined magnetic field and the inclination of the chain is enlarged by the gravitational force. These configurations of chains are approximately determined to minimize the total potential energy that consisted of the gravitational and magnetic potential energy. These characteristics were qualitatively confirmed by the numerical calculation with the two-dimensional Distinct Element Method. The investigation is expected to be utilized for the improvement of the two-component magnetic brush development system in electrophotography.

Journal of Imaging Science and Technology 46: 422–428 (2002)

Introduction

A magnetic brush development system in electrophotography process is shown in Fig. 1. Magnetic carrier beads with electrostatically attached toner particles are introduced into the vicinity of a rotatory sleeve with a stationary magnetic roller inside it.[1] Magnetized carrier beads form chain clusters on the sleeve in the magnetic field as shown in Fig. 2. Tips of chains touch the photoreceptor surface at the development area and toner particles on chains move to electrostatic latent images on the photoreceptor to form real images. Carrier chains play important roles in this development system in order to realize high quality imaging. Sufficient length and moderate stiffness of chains are required to obtain satisfactory image density and to prevent image defects. Therefore, it is necessary to clarify the relationship between kinetic characteristics of formed chains and design parameters, such as magnetic flux density and physical properties of carriers.

In these points of view, experimental and theoretical studies[2,3] have been reported on the magnetic interactions between magnetic particles. Numerical studies[4–6] have been also conducted using the Distinct Element Method (DEM)[7] to clarify detailed behaviors of particles in the development system. However, the mechanism of the chain forming process and the effect of design parameters have not been investigated systematically. In this study, parametric experiments using a solenoid coil as a source of magnetic field had been performed and a numerical simulation based on the DEM was conducted to clarify the statics of chains. Then, the results were discussed in the point of potential energy minimization.

Experimental

An experimental setup is illustrated in Fig. 3. Spherical soft magnetic particles (Toda Kogyo Corp.) shown in Fig. 4 were provided in the area with 10 mm in diameter at the center of the end plate on the solenoid coil. Magnetic particles made by the polymerization method are 18, 35, 55, 88 and 107 μm in average diameter, 3550 kg/m³ in volume density. Relative magnetic permeability obtained from the magnetization curve for the aggregate of particles is 4.34. Chains of magnetic particles formed in the magnetic field were observed and recorded by a digital microscope (Keyence Corp., VH-7000). Lengths and slant angles of chains were measured on the stored still images.

From the measured and numerically calculated results, axial magnetic flux density B''along the center axis of the coil can be approximated well by $B'(z) = B_0(1 - cz)$, where B_0 and $c = 66.87\ \mathrm{m}^{-1}$ are constants and z (m), $z = 0$ on the end plate of the solenoid coil, is the axial coordinate. Maximum magnetic flux density B_0 is proportional to the coil current with a proportional constant 0.00616 T/A.

Figure 5 shows the examples of observed chain profiles of 88 μm particles. In Fig. 5 (a) with coil current 1 A, and surface loading of particles per unit area 0.13 kg/m², chain formation was not clearly observed. However, a lot of thin and long chains were formed in (b) with increased coil current 3 A. Although the magnetic field intensity was common, chains became thicker and longer in (c) when the surface loading was increased from 0.13 to 0.25 kg/m².

Original manuscript received February 20, 2002

✦ IS&T Fellow

Nobuyuki.Nakayama@fujixerox.co.jp

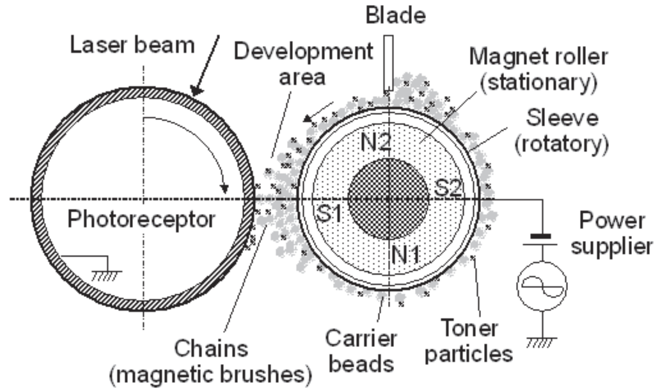

Figure 1. Magnetic brush development system.

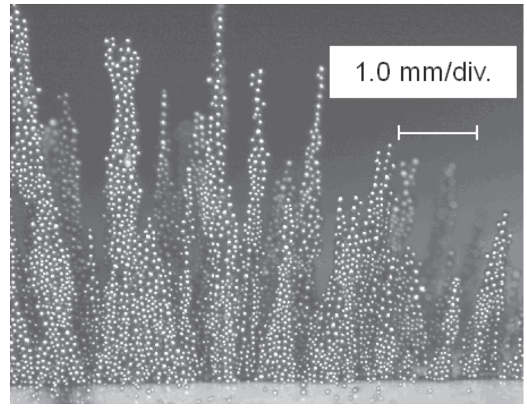

Figure 2. Chains of magnetic particles in magnetic field.

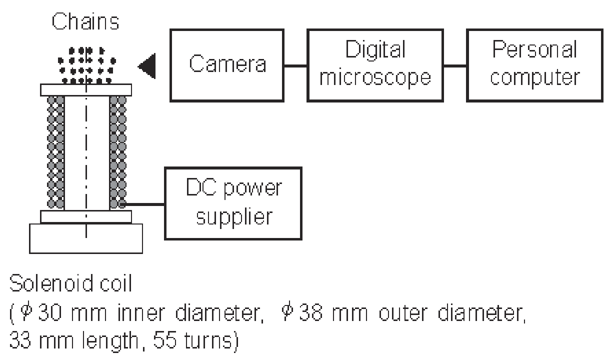

Figure 3. Experimental setup to measure lengths and slant angles of chains.

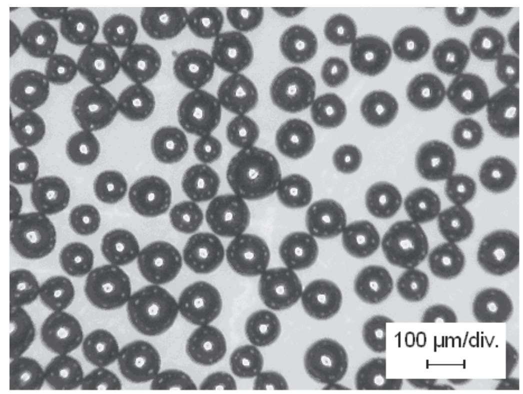

Figure 4. Photograph of magnetic particles with 107 μm in diameter. Spherical soft magnetic particles were used in the experiment.

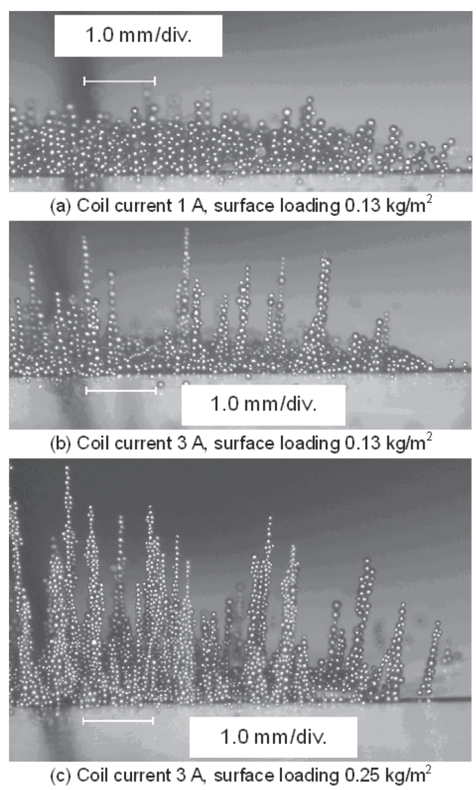

Figure 5. Observed chain profiles of 88 μm particles.

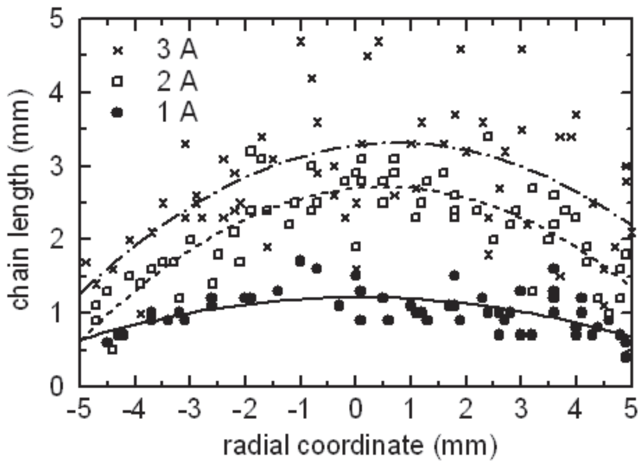

Figure 6. Measured chain length at various coil current (88 μm, 0.38 kg/m²).

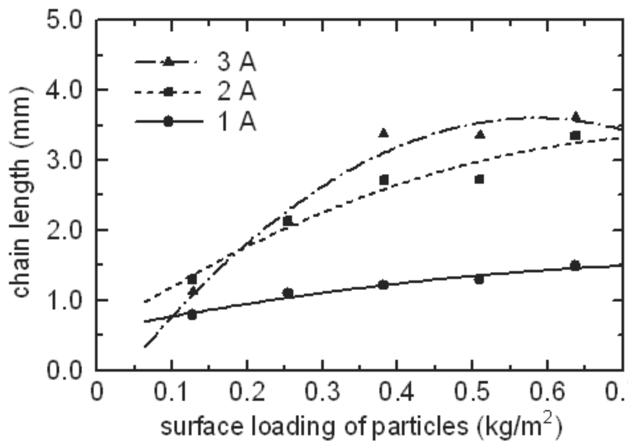

Figure 7. Relation between chain length and surface loading of particles (88 μm).

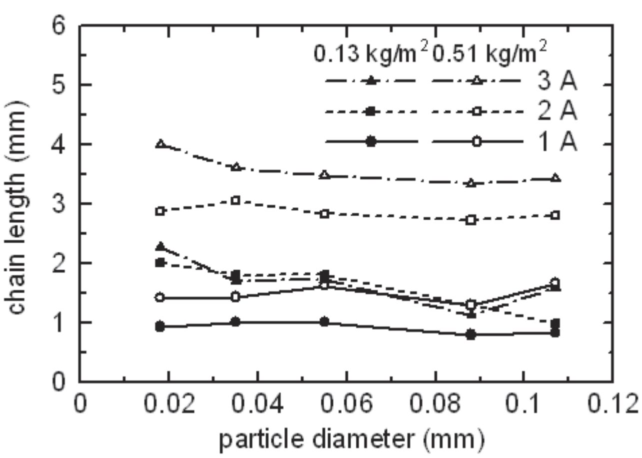

Figure 8. Relation between chain length and particle diameter.

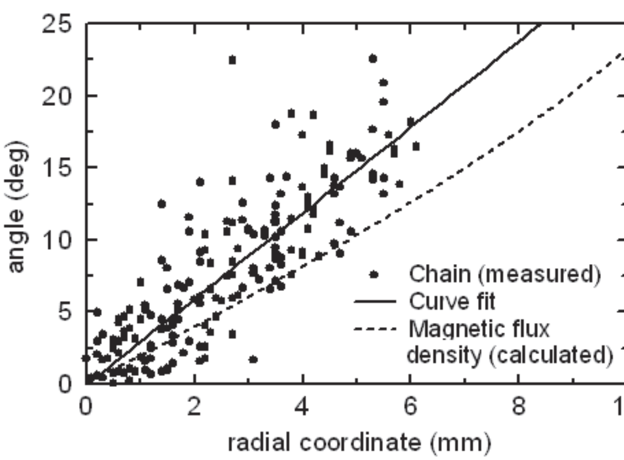

Figure 9. Relation between chain angle and radial coordinate.

Measured chain lengths of 88 μm particles were plotted in Fig. 6 as a function of the radial coordinate on the coil. While the length of each chain varies widely, the second order regression curves show clearly the dependency of the length on the coil current and the radial coordinate. The dependency on the coil current and the radial coordinate supposed to be equivalent to the dependency on the magnetic field. In Fig. 7, chain lengths at the center of the coil were plotted as a function of the surface loading. Chain length increases with the increase in the surface loading and the coil current. The relations between the chain length and the particle diameter are shown in Fig. 8. In the figure, chain lengths at various coil current and surface loading are plotted as a function of the particle diameter. It is shown that the smaller diameter of particles gives slightly longer chain length for smaller surface loading of particles, however if the surface loading of particles is large the length is almost independent of the particle diameter.

Slant angles of chains are plotted in Fig. 9 as a function of the radial coordinate with the calculated angle of the magnetic flux density. The angles increase linearly with the increase in the radial coordinate. Observed angles of chains are larger than that of the magnetic flux density. It is supposed that the gravity enlarged the slant angle.

Numerical Simulation

Numerical simulation was performed on chain forming process based on the two-dimensional DEM.[7] In the calculation the following momentum equations are solved for each particle with three degrees of freedom including rotation.

$$m_j \ddot{\mathbf{u}}_j = \mathbf{F}_j, \quad I_j \ddot{\varphi}_j = M_j, \tag{1}$$

where m_j, $\boldsymbol{u}_j$, I_j, ϕ_j, $\boldsymbol{F}_j$, M_j are mass, displacement vector, moment of inertia, rotation angle, applied force vector and moment applied to a particle j, respectively.

In this study, mechanical interaction force, magnetic force, air drag, and gravitational force are included in the equations. The mechanical interaction force in normal direction at the contact point was estimated from Hertzian contact theory. The interaction force in tangential direction was assumed proportional to the normal force with a proportional constant 0.25. The effect of rolling friction, van der Waals force and electrostatic force were neglected.

The magnetic force $\boldsymbol{F}_{mj}$ and rotational moment $\boldsymbol{M}_{mj}$ of the j-th particle with the magnetic moment $\boldsymbol{p}_j$ are given by the following expressions under the assumption that each particle behaves as a magnetic dipole placed at the center of the magnetized particle.[2]

$$\boldsymbol{F}_{mj}\ \ \boldsymbol{p}_j\ \ \cdot\nabla\boldsymbol{B}_j,\ \boldsymbol{M}_{mj} = \boldsymbol{p}_j \times \boldsymbol{B}_j \tag{2}$$

The magnetic moment $\boldsymbol{p}_j$ and magnetic flux density $\boldsymbol{B}_j$ at the position of the j-th particle are

$$\mathbf{B}_j = \mathbf{B}_j{}' + \sum_{\substack{k=1\\ j\neq k}}^{N} \mathbf{B}_{kj}, \tag{3}$$

$$\mathbf{p}_j = \frac{4\pi}{\mu_0}\frac{\mu-1}{\mu+2}\frac{a_j{}^3}{8}\mathbf{B}_j, \tag{4}$$

where N is the number of the particles, μ_0 is the permeability of free space, μ is the relative permeability of particles, a_j is the diameter of the j-th particle. The first term in the right hand side of Eq. 3 is the applied magnetic field by the coil and the second term is the field at the j-th particle due to dipoles of the other particles. $\boldsymbol{B}_{kj}$ is given by

$$\mathbf{B}_{kj} = \frac{\mu_0}{4\pi}\left(\frac{3\mathbf{p}_k \cdot r_{kj}}{\left|r_{kj}\right|^5} r_{kj} - \frac{\mathbf{p}_k}{\left|r_{kj}\right|^3}\right), \tag{5}$$

where $\boldsymbol{r}_{kj}$ is the position vector from the k-th to the j-th particle. The magnetic force is determined by solving Eqs. 3, 4 and 5 simultaneously and by substituting the calculated results, $\boldsymbol{p}_j$ and $\boldsymbol{B}_j$, to Eq. 2.

Simulated chain forming process is shown in Fig. 10. Initially, 225 particles were placed at random positions in the area with 5 mm in width and 8 mm in height as is shown in Fig. 10 (a). The number of particles was estimated from the surface loading of magnetic particles used in the experiment. (The number of 225 particles in this simulation is equivalent to 0.64 kg/m^2 in the experiment.) Young's modulus of the particles was assumed to be 10 GPa and that of the wall and the floor was assumed to be 100 GPa. Poisson's ratio and the friction coefficient were assumed to be 0.3 and 0.2, respectively. The motion of each particle was calculated every 100 ns after applying the gravitational field and the magnetic field equivalent to coil current 3 A that corresponds to the maximum magnetic flux density 0.0185 T.

In the simulated chain forming process shown in Fig. 10, discretely placed particles form clusters connected in lines first, then the clusters fall on the floor and grow up to treelike chains. It is also observed that the magnetic interaction forces applied to particles increase with the growth of chain length. It is clearly recognized that the calculated profile was similar to that in the experimental observations shown in Fig. 5.

Calculated dependency of maximum chain lengths on the surface loading of particles and the coil current is plotted in Fig. 11. Calculated results qualitatively agreed with the measured results shown in Fig. 7. That is, the chain becomes longer with the larger number of magnetic particles in the field of the higher magnetic flux density. However, the simulated results give smaller values of the chain length than the experimental results. One of possible reasons is that particles are apt to fall off chains in the simulation because of the neglected rolling friction. In addition to consideration of the rolling friction, three-dimensional DEM calculation is necessary to improve the quantitative accuracy. Additionally, it is supposed that the number of particles assumed in the calculation should be increased as is discussed in the later section.

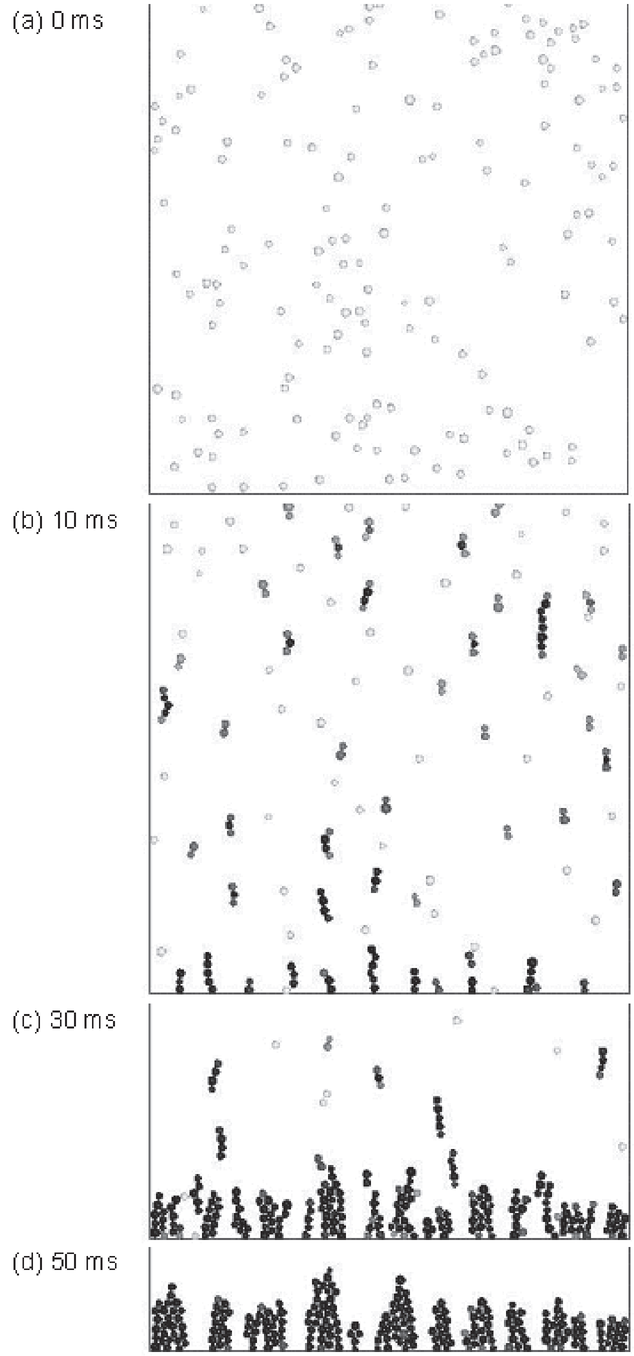

Figure 10. Simulated chain forming process by Distinct Element Method. Image density of particles designates magnitude of applied force.

Theoretical Discussion

We assumed the hypothesis that the chain length is determined to minimize its total potential energy. The to-

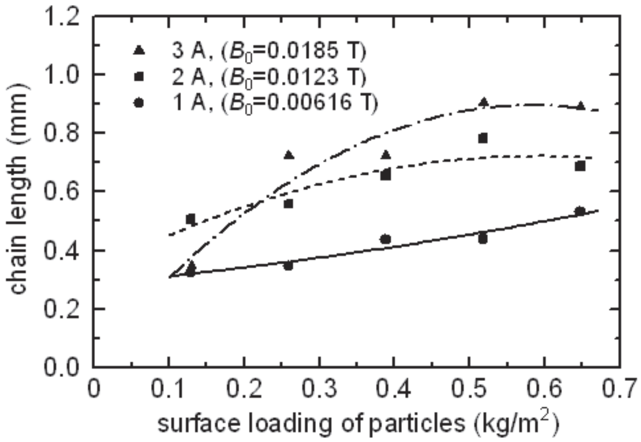

Figure 11. Calculated relations between chain length and surface loading of particles.

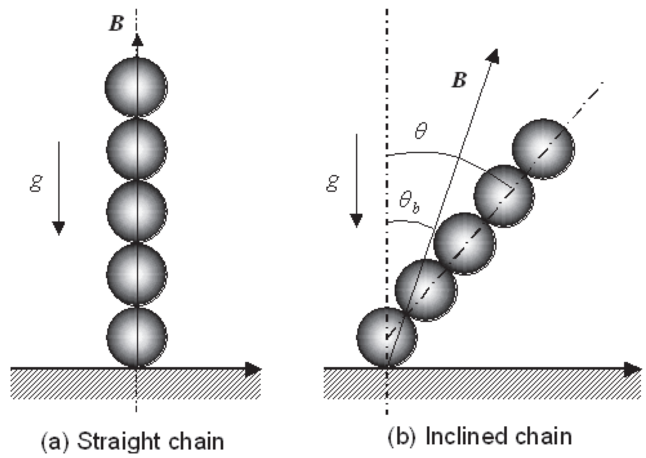

Figure 12. Schematic diagram of straight and inclined chain.

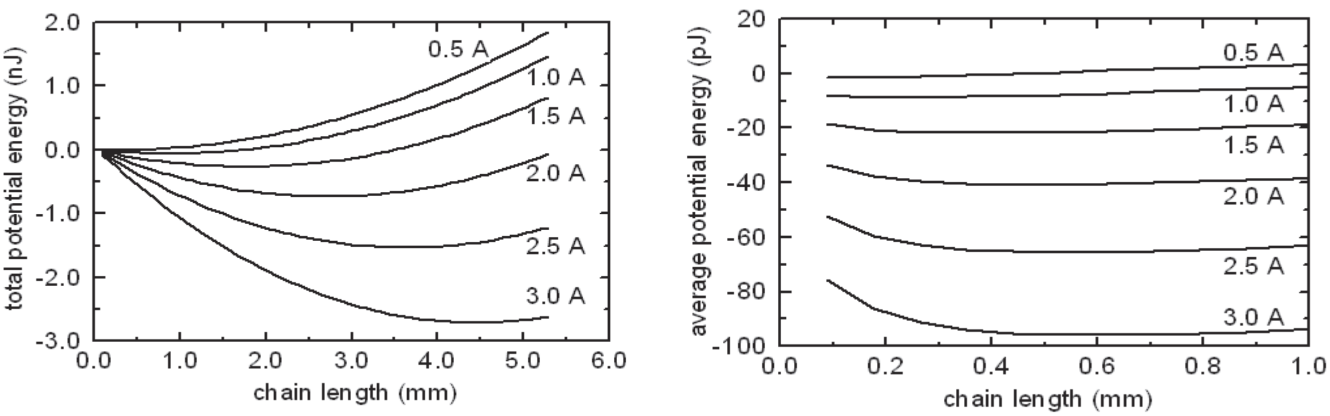

(a) Total potential energy

(b) Average potential energy

Figure 13. Calculated relations between potential energy and chain length.

tal potential energy is given by the sum of magnetic energy U_m expressed by Eq. 6 and gravitational energy.

$$U_m = -\frac{1}{2}\sum_{j=1}^{N} \mathbf{p}_j \cdot \mathbf{B}_j{}'. \tag{6}$$

On the assumption that particles are connected along a straight line in vertical direction, as illustrated in Fig. 12 (a), the relation between the chain length and the magnetic energy was calculated by solving Eqs. 3, 4 and 5. The gravitational energy is simply determined from the chain configuration. Calculated results are shown in Fig. 13. In the figure, both the total energy and the average energy are plotted for each coil current. The most stable chain length to minimize the energy exists for each coil current and the length increases with the increase in the coil current. It is also shown that the most stable length to minimize the total energy is different from that to minimize the average energy.

The calculated relations between the most stable chain length and coil current are plotted in Fig. 14 with experimental results and numerically simulated results. Figure 14(a) is the results for 88 μm particle and (b) is for 18 μm particle. Solid line describes the relation between the coil current and the chain length, l_t, to minimize the total energy, and the broken line describes the relation between the coil current and the chain length, l_a, to minimize average energy. Numerical results for surface loading 0.64 kg/m^2 are plotted by dot-dash lines.

In Fig. 14(a) for 88 μm particles, the experimental values are close to l_a with smaller number of particles, on the other hand, the values are close to l_t with larger number of particles. The theoretically estimated length l_t agrees with the experimental results for over 0.38 kg/m^2 particles. It suggests that the chain length is determined to minimize the total potential energy if sufficient particles to form chains are provided. However, if the number of particles is limited, the length is determined to minimize the average potential energy.

In Fig. 14(b), the theoretically estimated lengths of 18 μm particles are almost same as those of 88 μm particles. Although the experimentally measured lengths for smaller surface loading of particles are larger than those in Fig. 14(a), the lengths for larger surface loading of particles are almost same as those of 88 μm particles and theoretical values, l_t. The difference in the

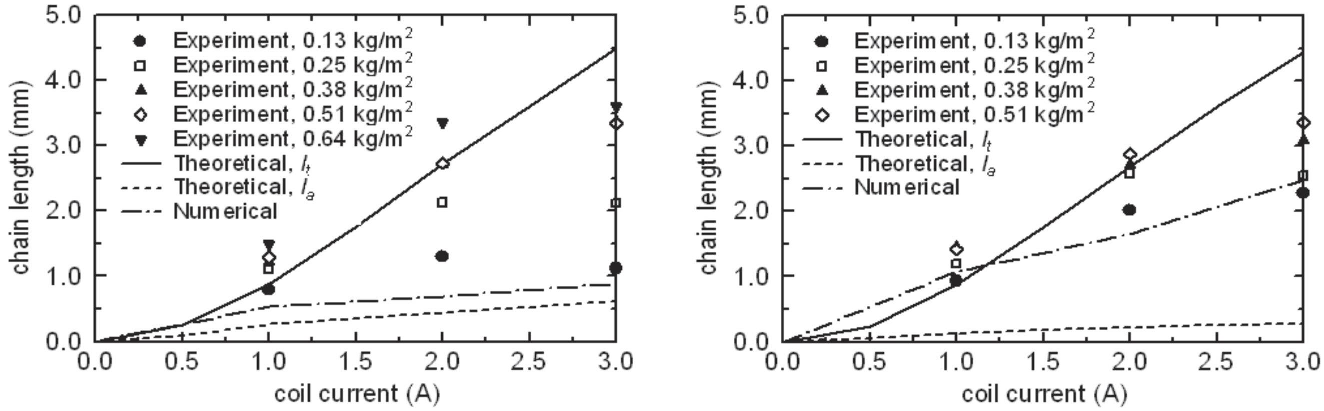

(a) 88 μm particles

(b) 18 μm particles

Figure 14. Comparison of calculated chain lengths with experimental results.

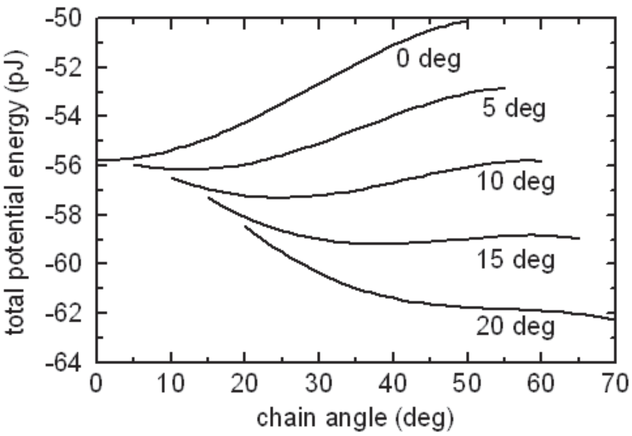

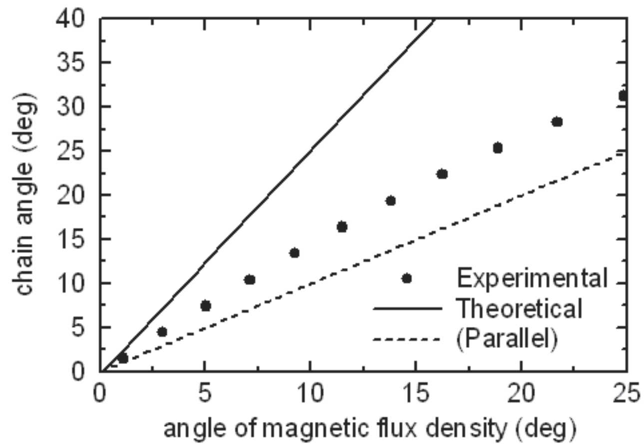

Figure 15. Effect of magnetic flux angle on the relation between potential energy and chain angle.

Figure 16. Comparison of calculated and experimental results of chain angle.

experimental results with particle diameter can be explained as the difference of number of particles.

On the other hand, numerical results for surface loading 0.64 kg/m^2 are close to the experimental results of surface loading 0.13 kg/m^2. These results suggest that numbers of particles assumed in the calculations are not equivalent to the experimental condition. The reason is supposed that the particles were gathered to the center of the coil in the experiment because the magnetic field is larger in the center of the coil. Non-uniformities of particle population and/or magnetic flux density must be considered for more realistic numerical calculation.

It is supposed that the slant angle of the chain is also determined to minimize the potential energy. The estimated total potential energy of the inclined chain, as is described in Fig. 12 (b), are plotted in Fig. 15 as a function of the chain angle, θ, for different angles of magnetic flux density, θ_b. Nine particles are assumed in this energy estimation. They minimize the total potential energy under the condition of coil current 1 A. It is shown that the most stable angle of chain exists for each angle of magnetic flux density if the angle is less than 20 degrees.

The most stable chain angle is plotted in Fig. 16 compared with the experimental result. The symbols express the relation between regression curve of the measured chain angle and calculated angle of magnetic flux density described in Fig. 9. A solid line expresses the theoretical results obtained from Fig. 15. It is confirmed that the gravitational field magnifies the chain angle. However the theoretically estimated chain angle is larger than the experimental result. A non-conservative theory must be established to quantitatively evaluate this phenomenon.

Conclusions

Lengths and slant angles of magnetic bead chains formed on the solenoid coil were measured to clarify the statics of chains and the chain forming mechanism. Motions of particles were numerically simulated using DEM and calculated results were compared with experimental results. Then, the stable conditions of chains were discussed in a viewpoint of potential energy minimization. It was clarified in the experimental observations that the chain length increases with the increase in magnetic flux density and the surface loading of particles but the chain length is independent of particle diameter if sufficient particles are provided. The chain forming process and these characteristics on the chain length were simulated by the two-dimensional DEM. It was also clarified that the slant angle of an inclined chain formed in the inclined magnetic field was enlarged by the gravitational force. These static conditions of chains are approximately determined to minimize the total potential energy that consists of the magnetic and gravitational energy. The present investigation is expected to be utilized for the improvement of the two-component magnetic blush development system.

Acknowledgement. The authors would like to express their thanks to Toda Kogyo Corp. for supplying magnetic particles, to Janjomsuke Wiphut (Bank of Thailand), N. Sukou, S. Yamada, and A. Sasakawa (Waseda Univ.) for their help of carrying out experiments. They also thank to the Ministry of Education, Culture, Sports, Science and Technology of Japan, Japan Society for the Promotion of Science, and The Okawa Foundation for Information and Telecommunications for the financial support.

References

1. E. M. Williams, *The Physics and Technology of Xerographic Processes*, Krieger Publishing, Florida, 1993.
2. R. S. Paranjpe and H. G. Elrod, Stability of chains of permeable spherical beads in an applied magnetic field, *J. Appl. Phys.* **60,** 418 (1986).
3. R. S. Paranjpe and H. G. Elrod, A magnetomechanical model of the magnetic brush, *J. Appl. Phys.* **63,** 2136 (1988).
4. Y. Shibata, J. Okuno, M. Kato, T. Aizawa, S. Tamura, and T. Iwai, Granular modeling coupled with the magnetic field, *Proceedings of Symposium on Computational Methods in Structural Engineering and Related Fields*, vol. 17, Japan Society of Steel Construction, Tokyo, 1993, p. 115.
5. S. Serizawa, Numerical simulation of carrier chain formation in magnetic brush development in electrophotography, *Japan Society of Mechanical Engineering D&D 99*, No. 99–7 (I), Japan Society of Mechanical Engineering, Tokyo, 1999, p. A228.
6. T. Kubota, H. Inoue, Y. Iino, and J. Hidaka, Numerical analysis for behavior of development in magnetic brush system of electrophotography by particles method, *Japan Hardcopy '99 Fall Meeting*, The Imaging Society of Japan, Tokyo, 1999, p. 26.
7. P. A. Cundall and O. D. L. Strack, A discrete numerical model for granular assemblies, *Géotechnique* **29,** 47 (1979).